

The second image (Fig. 3) tested is the eye-fundus blood vessels image (very few research reports about tracing eye-fundus blood vessels have appeared in the literature). Fig. 4 is the result of this tracing. Three blood vessels were tested, of which the trace starting points are labelled as *A*, *B* and *C*. When Figs. 3 and 4 are compared, the traced lines look fairly good. The crosses near *D* and *G* were processed successfully, but the branches near *E* and *F* were not detected. Other branches were successfully detected. By checking the Gaussian filter output, we find that zero-crosses were observed at those branches near *E* and *F*, implying that those branches were somehow cut by the filter (probably owing to noise), suggesting that zero-cross data only is not enough for boundary information.

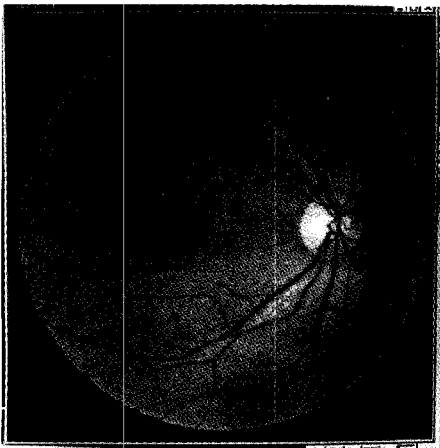


Fig. 3 Original fundus image

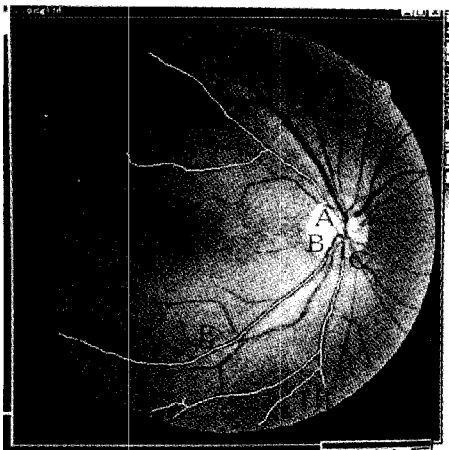


Fig. 4 Traced blood vessels of fundus image

Conclusions: A very simple algorithm is proposed to trace a maze or a blood vessel network. The idea comes from the navigational method of a bat. The experiments showed fairly good results. Since a human often uses a similar method when feeling his way in the dark, the method should be considered general. The advantage of this method is that information is obtained from many directions, rather than just from the right or the left. A more sophisticated algorithm could be developed using the idea, possibly combining some existing methods.

© IEE 1998

25 March 1998

Electronics Letters Online no: 19980689

T. Kurokawa, M. Kondoh, T. Oda and S. Kito (Department of Industrial Engineering, Aichi Institute of Technology, 1247 Yachigusa, Yagusa-cho, Toyota, 470-0356, Japan)

E-mail: kurokawa@ie.aitech.ac.jp

S.C. Lee (School of Electrical Engineering, The University of Oklahoma, 202 West Boyd, Room 219, Norman, Oklahoma 73019-0631, USA)

References

- 1 TAMURA, S., OKAMOTO, Y., and YANASHIMA, K.: 'Zero-crossing interval correction in tracing eye-fundus blood vessels', *Pattern Recognit.*, 1988, **21**, (3), pp. 227–233
- 2 LU, S., and EIHO, S.: 'Automatic detection of the coronary arterial contours with sub-branches from an x-ray angiogram'. Proc. Conf. Computers in Cardiology, 1993, pp. 575–578
- 3 LIU, L., and SUN, Y.: 'Recursive tracking of vascular networks in angiograms based on the detection-deletion scheme', *IEEE Trans. Med. Imaging*, 1993, **MI-12**, (2), pp. 334–341

Median-rational hybrid filters for image restoration

L. Khriji and M. Gabbouj

A new class of nonlinear filters is introduced, called median-rational hybrid filters (MRHFs), based on rational functions (RFs). The output is the result of rational operation taking into account three sub-functions. It is shown that every sub-function will preserve details within its sub-windows. The proposed MRHF filters have the inherent property that on smooth areas they provide good noise attenuation whereas on changing areas the noise attenuation is traded for good response to change. It is shown that a consistent reduction in the objectively measured mean absolute error and mean square error is obtained.

Introduction: The rational filter is one of the more recent and major classes of nonlinear filters. As the name indicates, it consists of a ratio of two polynomials. It is well-known that a rational function has several properties (it is a universal approximator and good extrapolator, can be trained using a linear algorithm, and requires lower degree terms than Volterra expansions) which can make it very effective in many signal processing tasks.

Rational function filters were used by Leung and Haykin [1] based on the work of Walsh [2] for signal detection and estimation, and were later applied by Ramponi in [3, 4] for image filtering and enhancement. This was later extended to deal with multidimensional data, in [5], for color image interpolation.

Specifically, in the image restoration problem, the rational filter developed in [3] performs well for relatively high SNR Gaussian contaminated environments. To derive a rational filter to deal with various kinds of noise such as Gaussian noise, impulsive noise and mixed (Gaussian/impulsive) noise, we propose a new class of nonlinear rational type hybrid filter for signal and image processing, median-rational hybrid filters (MRHFs). The MRH filter is based on three sub-operators in which the central sub-operator is a centre weighted median CWM filter acting on a plus-shaped mask.

One-dimensional median-rational hybrid filters: Consider the input vector $\mathbf{X}(\mathbf{n}) = [x(n-N), x(n-N+1), \dots, x(n-1), x(n), x(n+1), \dots, x(n+N)]$, which contains $(2N + 1)$ observation samples at each location \mathbf{n} . The output variable $y(n)$ is the result of a rational function using three input sub-functions which form an input vector $\Phi = [\Phi_1, \Phi_2, \Phi_3]^T$, where the 'central' sub-function Φ_2 is fixed as a centre weighted median filter. The proposed MRHF output is defined by

$$y(n) = \Phi_2(n) + \frac{\sum_{i=1}^3 \alpha_i \Phi_i(n)}{h + k(\Phi_1(n) - \Phi_3(n))^2} \quad (1)$$

where $\alpha = [\alpha_1, \alpha_2, \alpha_3]^T$ characterises the constant vector coefficients of the input subfunctions and satisfies the condition: $\sum_{i=1}^3 \alpha_i = 0$. In our study, $\alpha = [1, -2, 1]^T$. h and k are positive constants. The parameter k is used to control the size of the nonlinear effect.

The sub-filters Φ_1 and Φ_3 are chosen so that an acceptable compromise between noise reduction and edge preservation is obtained. It is easy to observe that this median-rational hybrid filter differs from a linear low-pass filter mainly in the scaling, which is introduced on Φ_1 and Φ_3 terms. Indeed, such terms are divided by a factor proportional to the output of an edge-sensing term characterised by $(\Phi_1(n) - \Phi_3(n))^2$. The weight of the median-operation output term is modified accordingly, in order to keep the gain

constant. The block scheme in Fig. 1a shows an example of the proposed one dimensional MRH filter structure, where Φ_1 , Φ_2 and Φ_3 are considered as three median sub-filters. Let us now examine its behaviour for different positive values of k .

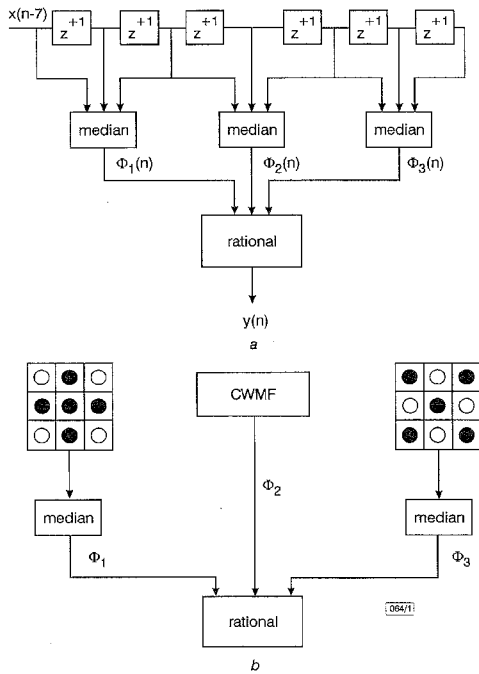


Fig. 1 Elements of 3×3 sliding window centred around pixel $x(n)$ for non-recursive implementation

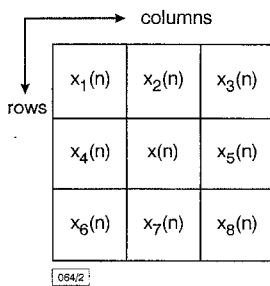


Fig. 2 Non-recursive 1D MRHF and 2D MRHF

a Example of non-recursive 1D MRH filter structure
 b Structure of 2D MRHF using two bidirectional median sub-filters

(i) $k \approx 0$, we obtain a linear relation between the three sub-filters cited above:

$$y(n) = \Phi_2(n) + \frac{\sum_{i=1}^3 \alpha_i \Phi_i(n)}{h} \quad (2)$$

(ii) $k \rightarrow \infty$, the output of the filter is identical to the central sub-filter output and the rational function has no effect:

$$y(n) = \Phi_2(n) \quad (3)$$

(iii) For intermediate values of k , the $(\Phi_1(n) - \Phi_3(n))^2$ term perceives the presence of a detail and accordingly reduces the smoothing effect of the operator

In this way, the MRH filter acts as a linear operator between three sub-operators, the coefficients of which are modulated by the edge-sensitive component.

Two dimensional median-rational hybrid filters: Consider the real-valued 2D sequence $\{x(\mathbf{n})\}$, and a 3×3 window centred around $x(\mathbf{n})$ given by Fig. 2 in order to filter the sample $x(\mathbf{n})$ at the central position. The three sub-filters $(\Phi_1(n), \Phi_2(n)$ and $\Phi_3(n)$ have the following forms:

(i) $\Phi_1(n)$ is a bidirectional median filter acting on the 'plus-shaped' mask.

(ii) $\Phi_2(n)$ is the output of a plus-shaped centre weighted median filter, which has the following filter window:

$$H = \begin{pmatrix} 0 & 1 & 0 \\ 1 & 3 & 1 \\ 0 & 1 & 0 \end{pmatrix}$$

(iii) $\Phi_3(n)$ is a bidirectional median filter acting on the 'cross-shaped' mask.

For the above MRHF structure, it was shown that every sub-filter will preserve signal details within their sub-windows. Hence, the MRHFs are very promising detail preserving filtering structures.

Experimental results: In order to objectively evaluate the performance of the MRHF, we have used the Lena image (512×512), and the following evaluation procedure. For this image, we have varied the corresponding parameter of the noise model (for the case of mixed noise (Gaussian with impulsive), only the variance of the Gaussian distribution was varied, and the percentage of impulses was constant and equal to 4%) and measured two performance measures: mean absolute error (MAE) and mean square error (MSE). The results obtained are shown in the form of plots in Figs. 3 – 5 for the three noise models: Gaussian (Fig. 3), impulsive (Fig. 4), and Gaussian mixed with impulsive (Fig. 5).

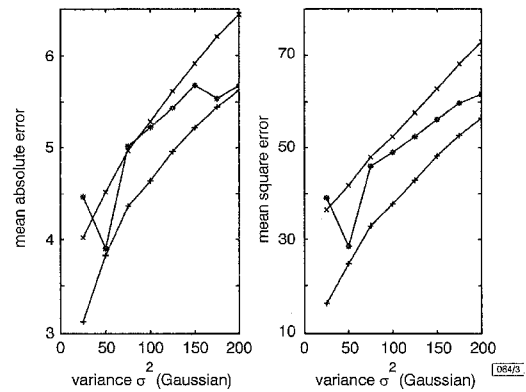


Fig. 3 Performance evaluation results for Gaussian noise

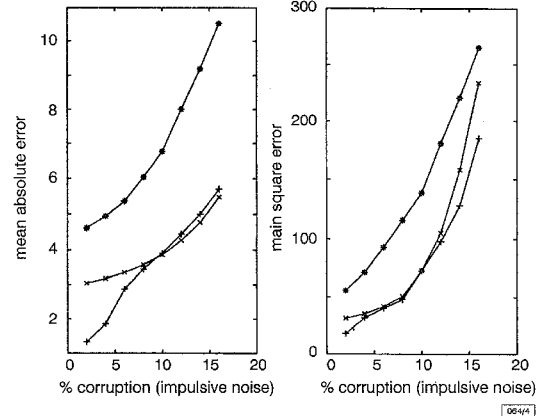


Fig. 4 Performance evaluation results for impulsive noise

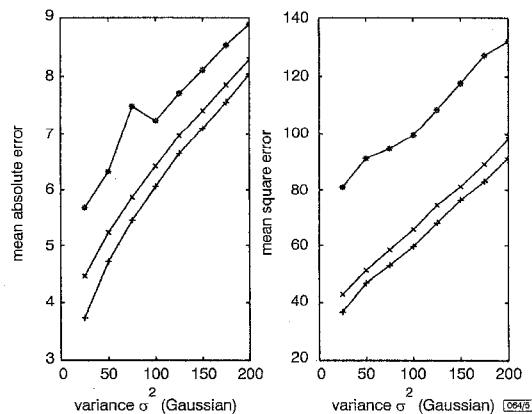


Fig. 5 Performance evaluation results for Gaussian mixed with 4% impulsive noise

As can be verified from Figs. 3 – 5, the performance of the MRHF is at least equal, and in most cases is superior, to the performance of the median filter and rational filter.

Conclusions: In this Letter, we have introduced a new class of nonlinear rational type hybrid filter for signal and image processing. The median-rational hybrid (MRH) filter is a rational function of three sub-filters in which the central filter is a CWMF. Experimental results demonstrated that the MRH filter can effectively remove various kinds of additive i.i.d. noise such as Gaussian noise, impulsive noise and mixed Gaussian-impulsive noise. Several nonlinear filters have also been tested and compared to our new MRH filters. In most cases, the MRH filter outperforms all the other filters for both of the objective criteria used.

Acknowledgment: This work has been supported by the European ESPRIT Project LTR 20229-Noblesse.

© IEE 1998

4 March 1998

Electronics Letters Online No: 19980666

L. Khrijji and M. Gabbouj (Signal Processing Laboratory, Tampere University of Technology, PO Box 553, FIN-33101 Tampere, Finland)

E-mail: lazhar@cs.tut.fi

References

- 1 LEUNG, H., and HAYKIN, S.: 'Detection and estimation using an adaptive rational function filter', *IEEE Trans. Signal Process.*, 1994, **SP-42**, (12), pp. 3336–3376
- 2 WALSH, J.L.: 'The existence of rational functions of best approximation', *Trans. Am. Math. Soc.*, 1931, **33**, pp. 668–689
- 3 RAMPONI, G.: 'The rational filter for image smoothing', *IEEE Signal Process. Lett.*, 1996, **3**, (3), pp. 63–65
- 4 RAMPONI, G.: 'Image processing using rational functions'. Proc. Cost 254 Workshop, Budapest, Hungary, 6–7 February 1997
- 5 CHEIKH, F.A., KHRIJJI, L., GABBOUJ, M., and RAMPONI, G.: 'Color image interpolation using vector rational filters'. Proc. SPIE Conf., Nonlinear Image Processing IX, San Jose, CA, 24–30 January 1998

Object oriented face detection using colour transformation and range segmentation

Sang-Hoon Kim, Hyoung-Gon Kim and Kyun-Hyon Tchah

A range segmentation technique using a matching pixel count (MPC) disparity histogram is combined with the generalised facial colour distribution (GFCD) skin-colour transform technique to provide robust multiple facial object detection with depth-range selectivity in a complex background environment.

Introduction: A number of representative studies have been carried out on face recognition, based on versatile techniques such as template matching [1] and elliptical k -means clustering [3]. However, these studies assume that the facial objects have already been isolated, which is, in fact, still an important problem in the face recognition field [2]. Recently, skin-colour information has been used to isolate facial objects from complex backgrounds [5]. However, there are problems when the background contains skin-like colours. Depth-based segmentation has been used for object-based coding of stereo image sequences [4].

This Letter proposes a novel object-oriented face detection algorithm using a skin-colour transform and range segmentation technique that can detect multiple facial objects according to their distance from the camera in a complex background environment. The skin-colour transform is defined with generalised facial colour distribution (GFCD), and the resulting image is combined with an efficient range segmentation technique which uses an MPC-based disparity histogram. This technique works well in various environments, because facial objects move as a whole and can be separated from the complex background without any ambiguity in the optically-based images. The overall block diagram of the proposed algorithm is shown in Fig. 1. The grabbed stereo image sequence

is used for range segmentation while the right image sequence is used for the skin-colour transform using GFCD. The two resulting images are fused together to define the final facial objects with a specific depth range.

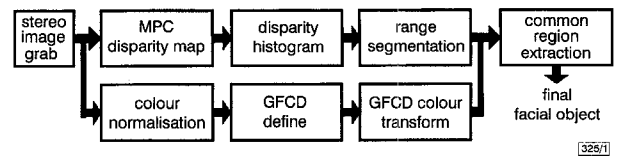


Fig. 1 Block diagram of proposed face detection algorithm

Object segmentation with MPC disparity histogram: As a preprocessing operation for the disparity map, LoG (Laplacian of Gaussian) is performed to enhance the edge information of the stereo images. Then a redundancy removed hierarchical area-based disparity operation is performed on these edge enhanced stereo image pairs for an efficient disparity map. Since conventional similarity measures like SAD (sum of absolute distance) and NCC (normalised correlation coefficient) have a boundary overreach problem along the object boundary, a new MPC similarity measure is introduced in this Letter. The disparity value $D(x, y)$ of the MPC disparity algorithm is defined as follows:

$$D(x, y) = \text{ARGmax}_d \sum_{x, y \in W} T(x, y, d) \quad (1)$$

$$T(x, y, d) = \begin{cases} 1 & |R(x, y) - L(x + d, y)| \leq V_{th} \\ 0 & \text{otherwise} \end{cases} \quad (2)$$

where W is a window for the similarity measure, d is the disparity search range, $R(x, y)$ is the pixel value of the right image at position (x, y) , $L(x+d, y)$ is the pixel value of the left image at position $(x+d, y)$ and V_{th} represents a predefined threshold value. The ARGmax_d operation selects d as $D(x, y)$ with maximum summation value, implying the most well matched position in the search range. This MPC-based disparity algorithm results in a correct object boundary because each pixel within the matching window has the same effect on the similarity measure. Table 1 summarised the performance of each similarity measure with the conventional SAD and NCC on the random-dot stereo images with varying salt-and-pepper noise. The resulting MPC disparity map is used for the calculation of the DH (disparity histogram), which is defined by the occurrence frequency of each disparity value. From the DH, the locations (depth range) and number of objects can be detected. The object segmentation process consists of the following steps: first, the outline of the DH curve is smoothed with average filtering. Next, regions with frequency values less than a specified threshold are forced to have zero frequency value. Continuous disparity values greater than the specified threshold represent objects with the same distance from the camera. Pixels with selected disparity values are extracted from the image, and each connected component (region) is assigned a unique label. Since the discontinuity of the disparity histogram usually corresponds to the natural object boundaries, a natural object-oriented segmentation of the scene is expected. The region with the smallest disparity value is regarded as the background.

Table 1: Summary of performance comparison of similarity measures with random-dot stereo image

Noise	Data	SAD	NCC	MPC
%				
0	Mis-pixels	1537	1662.1	1450
0	Matching ratio	94.55%	94.11%	94.86%
20	Mis-pixels	4535	11110	2208
20	Matching ratio	83.93%	60.64%	92.18%

Facial colour transform using GFCD: The right image of the stereo sequence is used for the skin-colour transform using facial color distribution. Since colour information is very sensitive to the brightness value of the pixel, each colour component is normalised with the brightness value. If $R(x, y)$, $G(x, y)$ and $B(x, y)$ are the colour component values of each pixel position (x, y) , the intensity of the pixel is given by $I(x, y) = R(x, y) + G(x, y) + B(x, y)$. The